Optics Communications 281 (2008) 4343–4347

Contents lists available at ScienceDirect

Optics Communications

journal homepage: www.elsevier.com/locate/optcom

Self-collimation and self-imaging effects in modulated waveguide arrays

S. Longhi [a,*], K. Staliunas [b,c]

[a] Dipartimento di Fisica and Istituto di Fotonica e, Nanotecnologie del Consiglio Nazionale delle Ricerche, Politecnico di Milano, Piazza L. da Vinci 32, I-20133 Milan, Italy
[b] Institucio Catalana de Reserca i Estudis Avancats (ICREA), E-08010 Barcelona, Spain
[c] Departament de Fisica i Enginyeria Nuclear, Universitat Politecnica de Catalunya, Colom 11, 08222 Terrassa, Spain

ARTICLE INFO

Article history:
Received 23 April 2008
Received in revised form 12 May 2008
Accepted 12 May 2008

PACS:
42.82.Et
42.79.Gn

Keywords:
Self-collimation in periodic dielectric media
Discrete diffraction in waveguide arrays
Dynamic localization

ABSTRACT

Self-collimation and self-imaging are comparatively investigated for discretized light in engineered modulated arrays of optical waveguides. It is shown that self-imaging is a rather extraordinary effect related to a fortuitous band collapse and it is thus rather distinct from self-collimation.

1. Introduction

In recent years, a great amount of theoretical and experimental studies have shown that the diffractive properties of light in periodically modulated dielectric media, such as in photonic crystals (PCs), arrays of evanescently-coupled waveguides and optically-induced lattices, are strongly affected by the complex spatial dispersive properties of the medium, with the relevant possibility of controlling the magnitude and sign of diffraction. Of particular interest is the self-collimation (or super-collimation) effect, by which an optical beam can propagate with almost no diffraction in a perfectly periodic (e.g. defect free) structure. The self-collimation effect, which has potential applications in optical integration of high-speed communication systems, was first predicted and observed by Kosaka et al. in a 3D PC [1], followed by other experiments (see, for instance [2–4]) till the recent demonstration of super-collimation over a huge propagation distance in a large area 2D PC with a square lattice of holes in air [5]. In such PC structures, self-collimation phenomena arise owing to the flattening of the isofrequency PC band surfaces at frequencies usually close to a band edge (see, for instance, [1,6,7]), strongly weakening the spatial dispersion for light waves.

Following the idea of diffraction management originally proposed and demonstrated in Ref. [8], diffraction control has been also extensively investigated and experimentally observed for discretized light in periodically-modulated arrays of evanescently coupled optical waveguides [9–17], including the occurrence of diffraction cancellation. Although diffraction cancellation (referred to as self-imaging or dynamic localization in Refs. [9–11,15]) in periodically-modulated waveguide arrays may bear a close connection with self-collimation phenomena in PCs and these two phenomena have been sometime referred using the same terminology [13,17], there are some differences, both conceptually and practically, that have been perhaps overlooked and that deserve to be clarified. In particular: (i) self-collimation is generally related to local flattening of a portion of the isofrequency curve in the reciprocal **k** space and thus diffraction cancellation occurs solely at low orders; conversely, self-imaging is a more stringent requirement as it implies diffraction suppression at *any* order and thus needs a full *collapse* of the quasi-energy band of the modulated array, (ii) self-imaging does not necessarily means beam spreading suppression at any distance, rather a periodic refocusing of the beam at the periodicity of the modulated array along the propagation direction, which may be larger than the diffraction length of the beam [11,12,15] and (iii) self-collimation is typically a non-resonant effect, whereas self-imaging it is.

As one might of course agree that self-imaging observed in Refs. [11,15] for discretized light is still an approximate effect (owing to

* Corresponding author. Tel.: +39 0223996160; fax: +39 0223996126.
E-mail address: stefano.longhi@fisi.polimini.it (S. Longhi).

0030-4018/$ - see front matter © 2008 Elsevier B.V. All rights reserved.
doi:10.1016/j.optcom.2008.05.014

such approximations as paraxiality, single-band or tight-binding assumptions, etc.), one must emphasize that band flattening requested for self-collimation is a rather common situation which is not necessarily related to (and does not imply) a full band collapse requested for self-imaging, which remains a rather extraordinary circumstance. This is explicitly shown in this work by comparing in detail the diffractive properties of two differently engineered modulated waveguide arrays, using in both cases the same degree of approximation in their analysis. The two structures, which have been previously considered in [9–11,15] and [14] as examples of engineered arrays for diffraction management, are schematically depicted in Fig. 1 and consist the former of an array of evanescently-coupled optical waveguides with a periodically-curved axis (Fig. 1a), the latter of a binary array of evanescently-coupled optical waveguides with a straight axis but with alternating and periodically varying waveguide width (Fig. 1b). Coupled mode-equations in the single-band, tight-binding and nearest neighbor approximations are used to describe discrete light diffraction in the two arrays according to Refs.[10,14]. For the array structure of Fig. 1(a), coupled equations for the mode amplitudes c_n trapped in the waveguides read [10,11]

$$\mathrm{i}\frac{\mathrm{d}c_n}{\mathrm{d}z} = -\Delta(c_{n+1} + c_{n-1}) + f(z)nc_n\,, \tag{1}$$

whereas for the array structure of Fig. 1b coupled-mode equations read [14]

$$\mathrm{i}\frac{\mathrm{d}c_n}{\mathrm{d}z} = -\Delta(c_{n+1} + c_{n-1}) + \frac{(-1)^n}{2}f(z)c_n. \tag{2}$$

In Eqs. (1) and (2), z is the paraxial propagation distance, 4Δ is the width of the tight-binding band of the array in absence of modulation, whereas $f(z)$ is a periodic function with period Λ and zero mean related to the local curvature of waveguides for the structure of Fig. 1a, and to the local propagation constant mismatch due to waveguide narrowing for the structure of Fig. 1b. Typically, we will consider a sinusoidal modulation as in Refs. [10] and [14]. Note that, after setting $c_n(z) = a_n(z)\exp[-\mathrm{i}n\int_0^z \mathrm{d}z' f(z')]$ in Eq. (1), and $c_n(z) = a_n(z)\exp[-(-1)^n \mathrm{i}\int_0^z \mathrm{d}z' f(z')/2]$ in Eq. (2), the following equivalent equations are obtained:

$$\mathrm{i}\frac{\mathrm{d}a_n}{\mathrm{d}z} = -\Delta(G^* a_{n+1} + G a_{n-1}), \tag{3}$$

for the structure of Fig. 1a, and

$$\mathrm{i}\frac{\mathrm{d}a_n}{\mathrm{d}z} = \begin{cases} -\Delta G(a_{n+1} + a_{n-1}) & n \text{ even} \\ -\Delta G^*(a_{n+1} + a_{n-1}) & n \text{ odd} \end{cases} \tag{4}$$

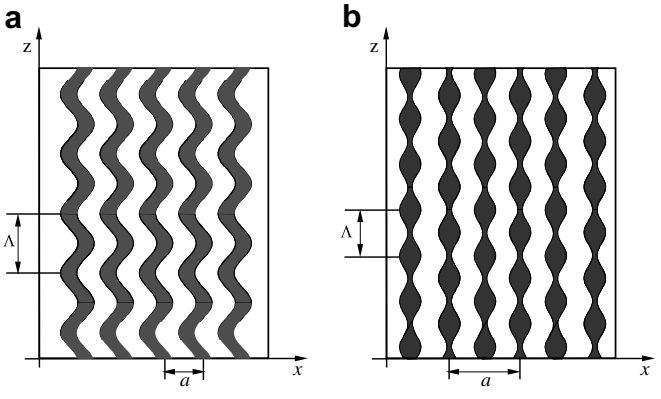

Fig. 1. Schematic of two modulated waveguide arrays for diffraction management: (a) array of waveguides with periodically-curved axis; (b) bi-periodic array of straight waveguides with periodically varying waveguide width.

for the structure of Fig. 1b, where we have set

$$G(z) \equiv \exp\left[i\int_0^z \mathrm{d}z' f(z')\right]. \tag{5}$$

Owing to the periodicity of coefficient G in Eqs. (3) and (4), Floquet theory applies and any solution to either Eq. (3) or Eq. (4) is given by an arbitrary linear superposition of Bloch-Floquet modes $c_n(z) = u_n(z,k_x)\exp[-\mathrm{i}\beta(k_x)z]$, which depend on the transverse wave number k_x, with k_x chosen in the first Brillouin zone $-\pi/a \leqslant k_x < \pi/a$. $u_n(z,k_x)$ is periodic in z with period Λ, whereas the Floquet exponent $\beta = \beta(k_x)$ represents the quasi-energy band of the periodically-modulated array (univocally defined apart from multiplies of the spatial modulation frequency $\omega = 2\pi/\Lambda$). Note that, as for the array of Fig. 1a one has solely one band $\beta(k_x)$, for the array of Fig. 1b one expects two bands $\beta_\pm(k_x)$ since we are dealing with a binary array. In absence of longitudinal modulation, i.e. for $f = 0$, for the array of Fig. 1a one obviously has $\beta(k_x) = -2\Delta\cos(k_x a)$ and $u_n(k_x) = \exp(-\mathrm{i}k_x na)$, whereas for the array of Fig. 1b one has $\beta_\pm(k_x) = \mp 2\Delta\cos(k_x a/2)$ with corresponding Bloch modes $u_n^+(k_x) = \exp(-\mathrm{i}k_x na/2)$ and $u_n^-(k_x) = (-1)^n\exp(-\mathrm{i}k_x na/2)$. The phenomena of self-collimation and self-imaging are related to the reshaping of the quasi-energy bands when the array is modulated along the longitudinal z-direction. If the spatial modulation frequency ω is larger than the waveguide coupling strength Δ, the flattening of the quasi-energy band $\beta = \beta(k_x)$ at around a given transverse wave number (for instance $k_x = 0$) corresponds to self-collimation. On the other hand, collapse of the quasi-energy band, i.e. the independence of $\beta(k_x)$ on k_x, corresponds to self-imaging (or dynamic localization, using a terminology drawn from solid-state physics), regardless of the spatial periodicity Λ of the modulation.

For the model (3), the quasi-energy band can be calculated in a closed form and is given by the relation (see, for instance, [18])

$$\begin{aligned}\beta(k_x) &= -2\Delta\,\frac{1}{\Lambda}\int_0^\Lambda \mathrm{d}z\,\cos\left(k_x a + \int_0^z \mathrm{d}z' f(z')\right) \\ &= -\frac{2\Delta}{\Lambda}Re\left\{\exp(\mathrm{i}k_x a)\int_0^\Lambda \mathrm{d}z G(z)\right\}\end{aligned} \tag{6}$$

Note that a band collapse, corresponding to $\partial\beta/\partial k_x = 0$, is attained whenever

$$\int_0^\Lambda \mathrm{d}z G(z) = \int_0^\Lambda \mathrm{d}z\exp\left[\mathrm{i}\int_0^z \mathrm{d}z' f(z')\right] = 0. \tag{7}$$

In particular, for a sinusoidal modulation $f(z) = A\cos(\omega z)$ one obtains the well-known result [19,20]

$$\beta(k_k) = -2\Delta J_0\left(\frac{A}{\omega}\right)\cos(k_x na), \tag{8}$$

i.e. the quasi-energy band has the same shape as that of the not modulated array, but with a width which is reduced from 4Δ to $4\Delta J_0(A/\omega)$. In particular, band collapse corresponding to self-imaging is attained whenever the ratio A/ω is a root of the Bessel function J_0. Therefore, for the model of Fig. 1a self-imaging is related to a shrinking of the quasi-energy band, which however is not deformed in shape by the modulation and remains sinusoidal [see Eq. (6)]. Obviously self-imaging leads to (exact) self-collimation for modulation frequencies ω larger than $\sim\Delta$.

Let us now consider the modulated binary array of Fig. 1b, for which self-collimation was previously predicted to occur in Ref.[14]. To compute the quasi-energy bands of the array, let us look for a solution to Eq. (4) of the form $a_{2n} = A(z)\exp(-\mathrm{i}k_x na)$, $a_{2n-1} = B(z)\exp(-\mathrm{i}k_x na + \mathrm{i}k_x a/2)$. One then obtains the following coupled equations for the amplitudes A and B

$$\mathrm{i}\frac{\mathrm{d}A}{\mathrm{d}z} = -\Delta_{k_x} G(z)B, \quad \mathrm{i}\frac{\mathrm{d}B}{\mathrm{d}z} = -\Delta_{k_x} G^*(z)A, \tag{9}$$

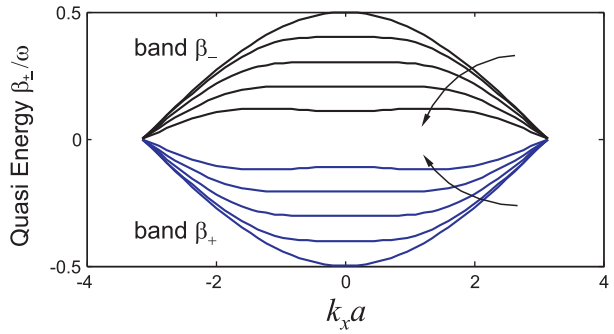

Fig. 2. Behavior of quasi-energies bands $\beta_{\pm}$ versus transverse wave number k_x for the modulated waveguide array of Fig. 1(b) for $\Delta/\omega = 0.25$ and for a few increasing values of normalized modulation amplitude A/ω. 0, 0.1, 0.2, 0.3 and 0.4. The arrows in the figure indicate the direction of increasing values of A/ω.

where we have set $\Delta_{k_x} \equiv 2\Delta\cos(k_x a/2)$. The solution to the periodic system (9) is of the form $(A(z), B(z))^{\mathrm{T}} = \exp(\mathscr{R}z)\Phi(z)(A(0), B(0))^{\mathrm{T}}$, where $\Phi(z)$ and $\mathscr{R}$ are two 2×2 matrices, with $\Phi(z+\Lambda) = \Phi(z)$ and $\Phi(z) = \mathscr{I}$. The quasi-energies $\beta_{\pm}(k_x)$ are then calculated as the eigenvalues of $\mathscr{R}$, which are the Floquet exponents for the system (9). It is easy to show that one has $\beta_-(k_x) = -\beta_+(k_x)$. The determination of the Floquet exponents can be done, in general, solely numerically. As an example, in Fig. 2 it is shown the behavior of the quasi-energy bands for a sinusoidal modulation $f(z) = A\cos(\omega z)$, for $\Delta/\omega = 0.25$ and for increasing values of A/ω. Note that a flattening of the quasi-energy band is observed near $k_x = 0$ for $A/\omega \sim 0.2 - 0.4$, which corresponds in fact to the regime of self-collimation previously considered in Ref.[14]. Now the main question can be stated as follows: is it possible for the structure of Fig. 1b a collapse of quasi-energy bands, which is more than simple band flattening? In other words: are the arrayed structures in Fig. 1 equivalent in terms of diffraction cancellation? The answer is negative, in the sense that even if the binary array of Fig. 1b permits self-collimation via band flattening, it is not a self-imaging structure because it shows *pseudo* collapses of quasi-energies, as we are going to demonstrate. Fig. 3 depicts, as an example, the detailed behavior of the allowed quasi-energies $\beta_{\pm}$ versus the ratio A/ω for a few values of the ratio Δ/ω. A shrinking of the quasi-energies is clearly observed for values of the ratio A/ω close to the roots of the Bessel function J_0, at least in the weak coupling limit where the ratio Δ/ω is small (see, for instance, Fig. 3c). However, an enlargement of the quasi-energies near such shrinking regions always reveals the presence of a pseudo collapse of the band (see, for instance, the inset of Fig. 3c). Owing to such a pseudo-collapse, suppression of discrete diffraction is therefore solely a first order (approximate) result for the structure of Fig.1b, whereas it is exact for the structure of Fig. 1a. In an experiment with waveguide arrays, this could be simply checked by imaging the flow of discretized light under single waveguide excitation at the input plane. Typical intensity light patterns that one would observe are shown in Fig. 4 for parameter values that may be typically achieved in practice ($\Lambda = 2$ mm , $\Delta = 0.3927\ \mathrm{mm}^{-1}$, and $A = 7.555\ \mathrm{mm}^{-1}$, corresponding to $\Delta/\omega = 0.125$ and $A/\omega = 2.405$). Note that, owing to the pseudocollapse (rather than a true collapse) of quasi-energies for the binary array structure, in Fig. 4b light does not remain confined in the excited waveguide, but clearly spreads into adjacent waveguides, whereas in Fig. 4a suppression of discrete diffraction is achieved.

One might argue that, for small values of the ratio Δ/ω, numerics may get inaccurate, and that an *exact* collapse might actually occur. This result might be naively suggested by the circumstance that, at very small values of the ratio Δ/ω, application of the averaging technique to Eq. (9) with rapidly-varying coefficients would lead to a set of equations analogous to Eq. (9) but with G replaced

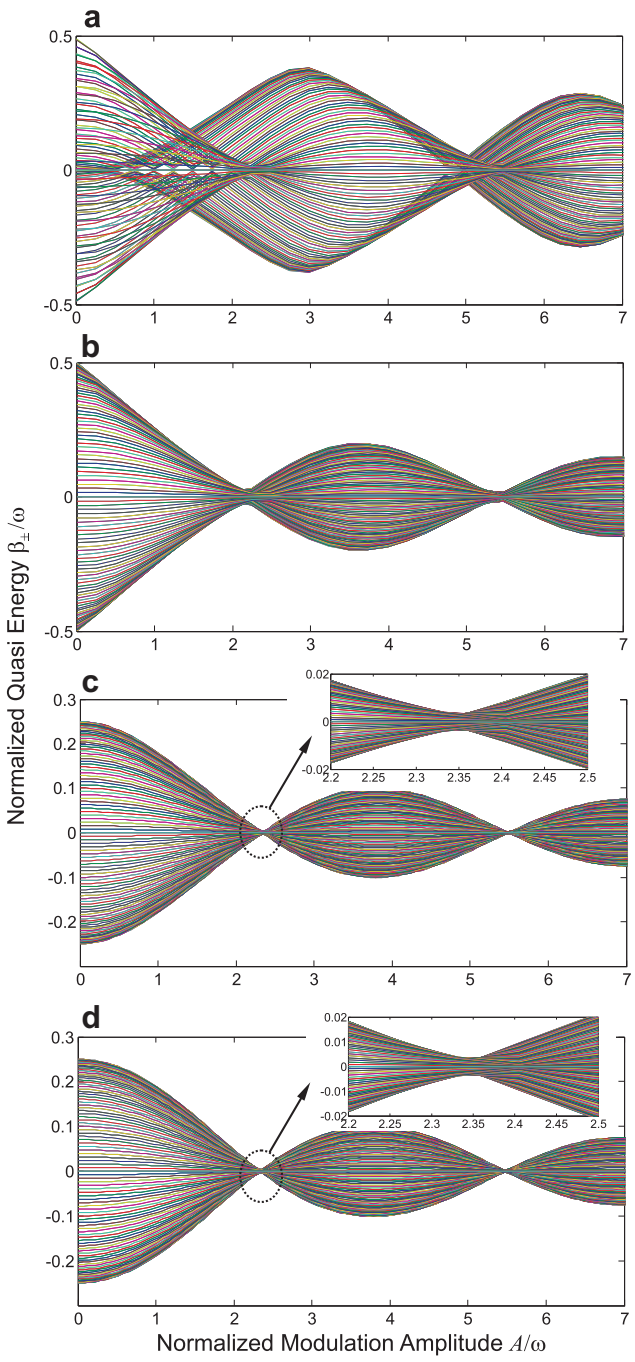

Fig. 3. (a)–(c) Numerically-computed quasi-energy spectrum $\beta_{\pm}/\omega$ in the first Brillouin zone for the modulated array of Fig. 1(b) as a function of the normalized modulation amplitude A/ω and for decreasing values of the ratio Δ/ω: (a) $\Delta/\omega = 0.5$; (b) $\Delta/\omega = 0.25$; (c) $\Delta/\omega = 0.125$. Figure (d) shows the quasi energy spectrum, corresponding to $\Delta/\omega = 0.125$ (the same as in Fig. 3(c)) as predicted by the asymptotic analysis (Eq. (19)). In (c) and (d) the enlargements show the details of the pseudo collapse that occur around the first zero of Bessel function J_0.

by its cycle-averaged value $\overline{G(z)} = J_0(A/\omega)$. A collapse of quasi-energies is thus expected at $J_0(A/\omega) = 0$. But this is an approximate result and a more appropriate asymptotic analysis is in order to capture the refined behavior of quasi-energies for small values of the ratio Δ/ω. To this aim, we perform a multiple scale asymptotic analysis of Eq. (9) assuming $\omega \sim O(1)$ (indeed, with a rescaling of z one can always assume $\omega = 1$) and $\Delta/\omega \sim O(\epsilon)$, where ϵ is a small parameter which organizes the asymptotic expansion (we will let $\epsilon = 1$ at the end of the calculations). Multiple scales for space are

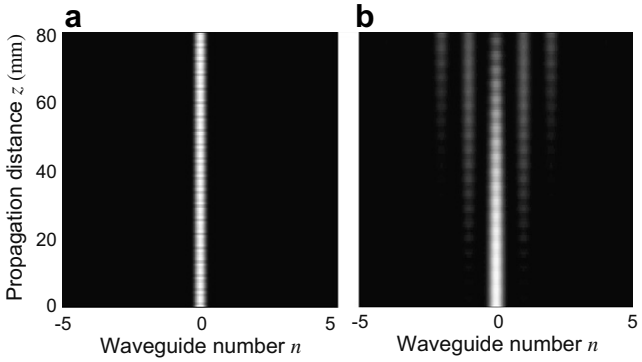

Fig. 4. Numerically-computed evolution of discrete light versus propagation distance under single waveguide input excitation for the modulated arrays of Fig. 1a and b [plots in (a) and (b), respectively] as predicted by coupled-mode Eqs. (1) and (2). Parameter values are given in the text and correspond to $\Delta/\omega = 0.125$ and $A/\omega = 2.405$.

introduced according to $Z_0 = z$, $Z_1 = \epsilon z$, $Z_2 = \epsilon^2 z$,... We then look for a solution to Eq. (9) in the form of power series

$$A = A^{(0)}(Z_0, Z_1, Z_2, \ldots) + \epsilon A^{(1)}(Z_0, Z_1, Z_2, \ldots) + \ldots$$
$$B = B^{(0)}(Z_0, Z_1, Z_2, \ldots) + \epsilon B^{(1)}(Z_0, Z_1, Z_2, \ldots) + \ldots \quad (10)$$

In developing the asymptotic analysis, it is worth writing the periodic function $G(z)$ as $G(z) = G_0 + \sum_{n\neq 0} G_n \exp(in\omega Z_0)$, where G_0 is the mean value of $G(z)$. For a sinusoidal modulation $f(z) = A\cos(\omega z)$, one has $G_n = J_n(A/\omega)$. The order of magnitude of G_0 as compared to ϵ is left undetermined at this stage, and hence we will write for the sake of convenience $G_0 = G_0^{(0)} + \epsilon G_0^{(1)} + \epsilon^2 G_0^{(2)} + \ldots$, where the only non-vanishing term in the expansion defines the order of magnitude of G_0. For instance, if A/ω is close to the first root of Bessel function in such a way that $J_0(A/\omega) \sim \epsilon^2$, we will set $G_0^{(n)} = 0$ for $n \neq 2$. After setting $\Delta_{k_x} = \epsilon q(k_x)$ with $q(k_x) = 2\cos(k_x a/2) \sim O(1)$ and using the derivative rule $\mathrm{d}/\mathrm{d}z = \partial_{Z_0} + \epsilon\partial_{Z_1} + \epsilon^2\partial_{Z_2}\ldots$, substitution of Eq. (10) into Eq. (9) yields a hierarchy of equations for successive corrections to A and B. At leading order $\sim \epsilon^0$, one simply obtains

$$A^{(0)} = F_1(Z_1, Z_2, \ldots), \quad B^{(0)} = F_2(Z_1, Z_2, \ldots) \quad (11)$$

where the amplitudes F_1 and F_2 vary over the slow spatial scales Z_1, Z_2,.... The evolution equations for F_1 and F_2 at the spatial scale Z_n is obtained from the solvability condition at order $O(\epsilon^n)$ in the asymptotic expansion. At order $O(\epsilon)$, for $G_0 \sim O(1)$ one obtains

$$\mathrm{i}\frac{\mathrm{d}A^{(1)}}{\mathrm{d}Z_0} = -\mathrm{i}\frac{\mathrm{d}A^{(0)}}{\mathrm{d}Z_1} - q(G_0^{(0)} + T)B^{(0)} \quad (12)$$
$$\mathrm{i}\frac{\mathrm{d}B^{(1)}}{\mathrm{d}Z_0} = -\mathrm{i}\frac{\mathrm{d}B^{(0)}}{\mathrm{d}Z_1} - q(G_0^{(0)*} + T^*)A^{(0)} \quad (13)$$

where we have set $T(Z_0) = \sum_{n\neq 0} G_n \exp(in\omega Z_0)$. The solvability condition at this order implies that the terms on the right hand sides in Eqs. (12) and (13) do not contain dc terms, i.e. one obtains

$$\mathrm{i}\frac{\partial F_1}{\partial Z_1} = -qG_0^{(0)}F_2, \quad \mathrm{i}\frac{\partial F_2}{\partial Z_1} = -qG_0^{(0)*}F_1. \quad (14)$$

Note that the asymptotic analysis can be stopped at this order provided that $G_0^{(0)} \neq 0$. For a sinusoidal modulation, this means that the ratio A/ω must be far enough from any root of J_0. In such a case, the quasi-energy bands are simply calculated as the eigenvalues associated to Eq. (14). For a sinusoidal modulation they read explicitly

$$\beta_\pm(k_x) = \mp 2\Delta J_0\left(\frac{A}{\omega}\right)\cos(k_x a/2). \quad (15)$$

Note that the two quasi-energy bands have the same shape as those of the not modulated array, apart from a reduction of the band width from 4Δ to $4\Delta J_0(A/\omega)$. This behavior closely resembles the one found for the modulated array of Fig. 1a [see Eq. (8)]. However, as Eq. (8) is an *exact* result, Eq. (15) is only *approximate* and, when A/ω gets close to any root of J_0, the asymptotic expansion must be pushed to higher orders because the evolution of amplitudes F_1 and F_2 occurs on the slower spatial scale Z_2. In such a case, assuming that $\sum_{n\neq 0}|G_n|^2/n = 0$, which holds for a sinusoidal modulation, at order $\sim \epsilon^2$ the solvability condition yields the following coupled equations

$$\mathrm{i}\frac{\partial F_1}{\partial Z_2} = -qG_0^{(1)}F_2, \quad \mathrm{i}\frac{\partial F_2}{\partial Z_2} = -qG_0^{(1)*}F_1 \quad (16)$$

which have the same form as Eq. (14). Therefore, for $G_0^{(1)} \neq 0$, the expression of the quasi-energies obtained by pushing the analysis at order $\sim \epsilon^2$ is again given by Eq. (15). For $G_0^{(1)} = 0$, i.e. when A/ω gets very close to any root of J_0 such that $J_0(A/\omega) \sim \epsilon^2$, the determination of the quasi-energies requires to push the asymptotic analysis to order ϵ^3. At such order, one can show that the solvability condition yields

$$\mathrm{i}\frac{\partial F_1}{\partial Z_3} = -q\left(G_0^{(2)} + \frac{q^2}{\omega^2}\Phi\right)F_2, \quad \mathrm{i}\frac{\partial F_2}{\partial Z_3} = -q\left(G_0^{(2)*} + \frac{q^2}{\omega^2}\Phi^*\right)F_1, \quad (17)$$

where we have set

$$\Phi \equiv \sum_{m,n\neq 0, m\neq n} \frac{G_m^* G_n G_{m-n}}{n(n-m)}. \quad (18)$$

The quasi-energies are then calculated as the eigenvalues of Eq. (17) and for a sinusoidal modulation read explicitly

$$\beta_\pm(k_x) = \mp 2\Delta\cos(k_x a/2)\left|J_0\left(\frac{A}{\omega}\right) + \frac{4\Delta^2}{\omega^2}\Phi\left(\frac{A}{\omega}\right)\cos^2(k_x a/2)\right| \quad (19)$$

where

$$\Phi\left(\frac{A}{\omega}\right) \equiv \sum_{m,n\neq 0, m\neq n} \frac{J_m(A/\omega)J_n(A/\omega)J_{m-n}(A/\omega)}{n(n-m)}. \quad (20)$$

Eq. (19), which very well reproduces the numerically-computed behavior of quasi-energies for $\Delta/\omega \ll 1$ (see Fig. 3d), clearly shows that there is solely a *pseudo-collapse* of the quasi-energy bands because at values $A/\omega \simeq 2.405,\ 5.520, \ldots$ (corresponding to one of the roots of Bessel function J_0) one has $\Phi(A/\omega) \neq 0$. It should also be noted that the occurrence of a pseudo-collapse for the waveguide array of Fig. 1b is expected to be a very general feature, i.e. quite independent of the specific modulation profile $f(z)$, because it is unlikely that the term Φ vanishes simultaneously with G_0. Even in this case, at higher-order spatial scales the collapse of quasi-energies is expected to be removed. In other words, band collapse (and hence self-imaging) found for model (1) represents a rather extraordinary circumstance which is not met in other models, such as in model (2) or in variations of them. For instance, the introduction of even small perturbations to model (1), such as non-neighboring coupling terms [15] or truncation effects [18], are known to make the collapse imperfect (at least for a general class of modulation profiles).

In conclusion, the phenomena of self-collimation and self-imaging for discretized light have been critically revisited by means of a comparative analysis of the diffractive properties of different arrayed waveguide structures recently proposed for diffraction management. The comparative study indicates that self-collimation is a much more common effect than self-imaging, the latter being an extraordinary effect which is a fortuitous event related to band collapse.

Acciones integradas HI-2005-0304 is gratefully acknowledged.

References

[1] H. Kosaka, T. Kawashima, A. Tomita, M. Notomi, T. Tamamura, T. Sato, S. Kawakami, Appl. Phys. Lett. 74 (1999) 1212.
[2] L.J. Wu, M. Mazilu, T.F. Krauss, J. Lightwave Technol. 21 (2003) 561.
[3] D.W. Prather, S.Y. Shi, D.M. Pustai, C.H. Chen, S. Venkataraman, A. Sharkawy, G.J. Schneider, J. Murakowski, Opt. Lett. 29 (2004) 50.
[4] Z. Lu, S. Shi, J.A. Murakowski, G.J. Schneider, C.A. Schuetz, D.W. Prather, Phys. Rev. Lett. 96 (2006) 173902.
[5] P.T. Rakich, M.S. Dahlem, S. Tandon, M. Ibanescu, M. Soljacic, G.S. Petrich, J.D. Joannopoulos, L.A. Kolodziejski, E.P. Ippen, Nat. Mater. 5 (2006) 93.
[6] J. Witzens, M. Loncar, A. Scherer, IEEE J. Sel. Topics Quantum Electron. 8 (2002) 1246.
[7] Y. Loiko, C. Serrat, R. Herrero, K. Staliunas, Opt. Commun. 269 (2007) 128.
[8] H.S. Eisenberg, Y. Silberberg, R. Morandotti, J.S. Aitchison, Phys. Rev. Lett. 85 (2000) 1863.
[9] G. Lenz, R. Parker, M.C. Wanke, C.M. de Sterke, Opt. Commun. 218 (2003) 87.
[10] S. Longhi, Opt. Lett. 30 (2005) 2137.
[11] S. Longhi, M. Marangoni, M. Lobino, R. Ramponi, P. Laporta, E. Cianci, V. Foglietti, Phys. Rev. Lett. 96 (2006) 243901.
[12] S. Longhi, M. Lobino, M. Marangoni, R. Ramponi, P. Laporta, E. Cianci, V. Foglietti, Phys. Rev. B 74 (2006) 155116.
[13] I.L. Garanovich, A.A. Sukhorukov, Yu.S. Kivshar, Phys. Rev. E 74 (2006) 066609.
[14] K. Staliunas, C. Masoller, Opt. Express 14 (2006) 10677.
[15] R. Iyer, J.S. Aitchison, J. Wan, M.M. Dignam, C.M. de Sterke, Opt. Express 15 (2007) 3212.
[16] I.L. Garanovich, A. Szameit, A.A. Sukhorukov, T. Pertsch, W. Krolikowski, S. Nolte, D. Neshev, A. Tuennermann, Y.S. Kivshar, Opt. Express. 15 (2007) 9737.
[17] I.L. Garanovich, A.A. Sukhorukov, Y.S. Kivshar, Opt. Express 15 (2007) 9547.
[18] M. Holthaus, D. Hone, Phys. Rev. B 47 (1993) 6499.
[19] D.H. Dunlap, V.M. Kenkre, Phys. Rev. B 34 (1986) 3625.
[20] M. Holthaus, Phys. Rev. Lett. 69 (1992) 351.